

An Analytical Study of Meteor Entry

JAMES A. FAY,* W. CRAIG MOFFATT,† AND RONALD F. PROBSTEN‡
Massachusetts Institute of Technology, Cambridge, Mass

The paper analyzes the problem of the convective and radiative heat transfer and the resultant ablation of meteors which enter the earth's atmosphere in the speed range of 20-70 km/sec and at relatively steep angles. Analytical estimates are obtained for the continuum radiative and continuum convective heating rates in multiply ionized gases assumed to be in thermochemical equilibrium. Shielding of both the convective and radiative heat transfer to the surface as a result of vaporizing ablation is considered. The conditions for peak heating of the meteor are shown to be related to those for peak deceleration. These conditions are related in turn to the heating rates and the meteor ballistic parameter, from which the mass of ablated material is then calculated. The results show that radiative heating will become more important than convective heating at altitudes below 25 km, at which point the shock layer is optically thin. Only for bodies having peak heating within a scale height above sea level will the gas cap become opaque, and in this region the diffuse radiation approximation for heat transfer is not applicable. It is also shown that nonvaporizing bodies will not survive with a small mass loss unless they are large enough to impact the earth before peak heating. Vaporizing bodies between a fraction of a centimeter and several centimeters in radius will survive with little change in mass, essentially independently of velocity or entry angle. If the ablation products are opaque to the gas-cap radiation, bodies larger than 0.5 m may also survive with little mass loss for entry speeds in the lower part of the range considered.

Nomenclature

A	= frontal area of meteor
c	= velocity of light
C_D	= drag coefficient of meteor (1 in present calculations)
C_p	= specific heat at constant pressure
e	= magnitude of electronic charge
f	= total heat transfer to meteor divided by QA
G	= function defined by Eq (A2)
h	= Planck's constant
Δh	= heat per unit mass required to vaporize the material or to melt it
H	= stagnation enthalpy behind detached shock
K	= thermal conductivity
k	= Boltzmann constant
K_R	= radiation thermal conductivity, Eq (A12)
l_p	= Planck mean free path for continuum radiation, Eq (A16)
l_R	= Rosseland mean free path for continuum radiation, Eq (A10)
l_v	= photon mean free path, Eq (A9)
l^*	= atmospheric scale height at peak heating altitude
m	= exponent of velocity in relation $\xi \propto \rho_\infty^{-n} V_\infty^{-m}$, Eq (2.8)
m	= electron mass
m_i	= ion mass
M	= mass of meteor (present calculations based on 3.2 g/cm ³ density)
ΔM	= ablated mass of meteor
n	= principal quantum number
n	= exponent of density in relation $\xi \propto \rho_\infty^{-n} V_\infty^{-m}$, Eq (2.8)
n	= electron number density, number/cm ³
n_i	= ion number density
n_m	= a minimum quantum number, Eq (A5)

p	= stagnation pressure
q	= stagnation-point heat-transfer rate (per unit area)
Q	= total heat transfer (per unit area) to stagnation point over meteor trajectory, Eq (2.11)
R	= body radius and/or local radius of curvature at stagnation point
t	= time of flight of meteor in atmosphere
T	= absolute temperature, °K
u	= velocity appearing in inviscid velocity gradient du/dx at stagnation point of body
V_∞	= meteor velocity
x	= parameter defined by Eq (A10)
x	= distance along body surface from stagnation point
y	= distance normal to body surface
z	= altitude
Z	= total molal concentration, Eq (3.2)
Z	= ionic charge in units of e (Appendix)
Z	= average ionic charge, Eq (3.2)
δ_T	= function of Z , Eq (4.13)
Δ	= shock-layer thickness at stagnation point and thickness of a thin transparent gas slab
ϵ	= density ratio across shock, ρ_∞/ρ_s
ϵ_r	= energy radiated per unit volume, time, and frequency
η	= quantity which measures blowing effect of ablating material, Eq (2.13)
η	= transformed y coordinate in boundary layer, Eq (4.4)
θ	= ratio of ion-electron recombination energy to kT , Eq (A3)
θ	= inclination angle of meteor trajectory with respect to horizontal
θ	= T/T
Λ	= Spitzer function defined by Eq (4.14)
ν	= frequency of radiation
ν_i	= ionization frequency, Eq (A4)
ξ	= ratio of stagnation-point heat-transfer rate q to energy flux in freestream $\frac{1}{2}\rho_\infty V_\infty^3$
ρ	= density
σ	= Stefan-Boltzmann constant
τ_v	= photon mean free time
ϕ	= modified ballistic parameter defined by Eq (2.5)

Subscripts

B	= with reference to blackbody radiative heating
c	= with reference to convective heating
i	= initial conditions on entry into atmosphere
R	= with reference to continuum transparent radiative heating

Presented as Preprint 63-451 at the AIAA Conference on Physics of Entry into Planetary Atmospheres, Cambridge, Mass., August 26-28, 1963; revision received February 7, 1964. The authors are indebted to Paul Croce for his aid in the numerical analysis. This work has been sponsored by the Advanced Research Projects Agency (Ballistic Missile Defense Office) and technically administered by the Fluid Dynamics Branch of the Office of Naval Research.

* Professor of Mechanical Engineering, Department of Mechanical Engineering. Member AIAA.

† Assistant Professor of Mechanical Engineering. Department of Mechanical Engineering. Member AIAA.

‡ Professor of Mechanical Engineering, Department of Mechanical Engineering. Fellow Member AIAA.

- s = stagnation conditions and/or conditions behind normal detached bow shock wave
 w = wall conditions
 ∞ = freestream conditions

Superscript

- * = conditions at peak heating

I Introduction

INTEREST in the entry of meteoroids§ into the earth's atmosphere by those engaged in vehicle planetary entry studies has stemmed from the recognition that meteor observations could possibly aid in the understanding of re-entry aerodynamic heating at very high speeds. Since it is presumed that meteoroids are of solar origin, then studies of the entry phenomena associated with such bodies should cover the speed range of interest for solar navigation. Furthermore, observations of meteors could provide information under speed and enthalpy conditions which are, today, not presently attainable under controlled laboratory conditions. These facts were recognized early and pointed out to those engaged in high-speed vehicle re-entry studies by Hansen¹ and Gazley.² However, these authors essentially considered only the smaller meteoric bodies in which the heating and ablation are associated with free molecule conditions, where the mean free path is large in comparison with the characteristic meteor dimension. An analysis of the heating and mass loss problem for meteors, which included both continuum convective heat transfer and gas radiation, along with conclusions regarding the vehicle re-entry problem, was given in a paper by Riddell and Winkler.³ However, both the convective and radiative heating rates that were used there are open to question for meteor entry at velocities exceeding 20 km/sec, where the air in the gas cap can be multiply ionized. Nevertheless, many of the general concepts introduced in this paper are of considerable interest.

Perhaps the clearest perspective of the status of the aerodynamic heating problem and the role it plays in the observation and survival of meteoric bodies has been presented in a series of papers by Allen.⁴⁻⁶ Again, however, the detailed heating considerations applied in these papers are applicable to the slower meteors so that their use in the range of higher-speed entry and the resulting conclusions which one can draw must be investigated.

In this paper the purpose of the authors is to analyze the problem of the convective and radiative heat transfer and the resultant ablation of meteors which enter the earth's atmosphere in the speed range of 20-70 km/sec. This latter speed is approximately the earth-approach speed which a body may have and still be a member of the solar system. In connection with the heating and ablation considerations, the restricted survival problem of determining the size of meteors that lose only a small fraction of their mass before impact will also be considered. Although no fundamentally new concepts are set forth, nevertheless certain ideas on radiative and convective heating in multiply ionized gases, not heretofore applied to the problem, are presented. The approach used permits an essentially analytical study, in contrast to most previous works, which are primarily numerical. In this way, the problem is readily put into a form where physical properties different from those employed here readily may be taken into account.

As is well known, meteoric bodies range in size from minute dust particles to asteroids, and the mode of convective heat transfer to these bodies will be determined by the characteristic size of the object in relation to the appropriate local mean free path of the surrounding atmosphere. In the present paper we shall be concerned only with the case of continuum

heat transfer, in which the appropriate mean free path is small in comparison with the characteristic length. As will be shown in the following section, an important quantity in determining meteor behavior and survival is the altitude and stagnation conditions for the peak rate of heat transfer to the body. The larger the size of the body when it enters the atmosphere, the lower will be the altitude at which the peak heating takes place. Now it can be shown that, for bodies whose characteristic dimension is larger than about 1 mm, this altitude for peak heating always occurs at a condition where the convective heat transfer is determined by continuum characteristics. We therefore shall not be concerned with free-molecule entry conditions, which, for the present paper, implies bodies whose size on entry is less than about 1 mm. We would point out, however, that it is only in the free-molecule case where the collision of the air molecules with the surface molecules is directly proportional to the rate of removal of mass, a common assumption made by meteor physicists.⁷

In the broad sense, all meteors survive to the earth. If they are large enough, the total amount of heating will have been insufficient to ablate the entire mass. On the other hand, if they are of an intermediate size, where appreciable mass loss takes place, eventually they will reach an equilibrium in a free-molecule condition, although they may be very small (clearly, smaller than the previously mentioned size of 1 mm). In our considerations of survival, we shall restrict our dynamical analysis to those meteors that lose only a small fraction of their total mass during entry, so that the meteor size remains essentially unaltered to impact. Such an analysis can be readily generalized to variable mass¶; however, it is felt that the present survival definition will cover a wide enough class of bodies, particularly those configurations of most interest to the re-entry vehicle designer.

The entry angle of a meteoroid into the earth's atmosphere can range from vertical to very shallow. Since most meteors enter at relatively steep angles, in the analysis which follows we shall make the assumption that the entry angle is steep. Such bodies experience high heating rates for times which are short in comparison with their atmospheric transit time.

In our analysis we shall consider the meteor to be essentially spherical. Allen⁴ has shown that a sphere is probably a good approximation for calculating the entry dynamics and heat transfer for most meteors. Although the density of the meteor is not known a priori, for purposes of illustration we shall here consider the meteor as having the density of stone. Iron meteors, having somewhat higher density, would not differ greatly in ballistic performance. The major difference between these materials is probably their ablation characteristics, and the ten-to-one preponderance of stonelike meteors falling to the earth's surface may reflect the difference in the dependence of the mass loss on the effects of vaporization.

Perhaps the strongest restriction to be placed on the calculation of the appropriate thermal properties and convective and radiative heat transfer is the assumption that the flow is in thermodynamic and chemical equilibrium. For the peak heating altitudes considered, where the flow can be treated as a continuum, the assumption may be a reasonable one.

Because the peak heating rates are so large, the heat input to the body is taken to appear as ablation of the surface, and the internal temperature of the body is assumed to remain essentially unchanged. Allen⁶ has pointed out, however, that the stonelike materials, because of their low thermal

§ A meteoroid becomes a meteor on entering the atmosphere and a meteorite when it strikes the earth's surface.

¶ Such calculations are being carried out by one of the present authors (W. C. Moffatt). The assumption of a constant body size leads to somewhat increased heat transfer rates, and therefore somewhat larger body sizes can survive. The overall results and trends of the present analysis are not expected to be changed.

conductivity, may not be able to withstand the high surface thermal stresses resulting from the heating rates and, as a result, may spall. In this case, not only will vaporization not occur but some of the material could enter the boundary layer in the solid state without having been heated. This type of local failure can be progressive, a condition which in fact seems to be a common occurrence with large stony meteors and results in meteor flaring. We will not attempt to answer the question of spalling here, and we will assume, for lack of more detailed information, that the ablation limits are defined by melting on the one hand, and vaporization on the other. The actual convective heating mode is taken to be laminar, since the Reynolds numbers at peak heating are generally very low.

Finally, we shall make several assumptions regarding radiative heat transfer. In the first place, we take the radiative heat transfer from the body to be small in comparison with the heat transferred to it. This is easily shown to be the case for the present problem. Furthermore, the radiation cooling behind the shock wave is considered sufficiently small so that we may apply the Hugoniot conditions there. This assumption is also readily justified from the results. So far as the radiant heat transfer from the gas cap to the body is concerned, this heat transfer is taken to be that associated with the air alone and not the vapor or even possibly solid particles themselves. As two limits which would correspond to "radiation blowing" we will consider the material in the vapor state from the body as leaving the opacity of the medium unaltered on the one hand and on the other making the boundary layer opaque. The ablated material is assumed not to be excited sufficiently so as to materially increase the radiative heat input to the body.** Although the calculations will be carried out for continuum radiation, a comparison with appropriate line radiation estimates will be made.

II Integrated Heat Transfer and Ablated Mass

An estimate of the total heat transfer to a body entering the earth's atmosphere at steep angles can be made by noticing that the heat-transfer rate reaches a local peak at the point where the decreasing velocity more than counterbalances the effect of the increasing density (see, e.g., Ref 8, p. 7), and that the heating rate may be integrated on either side of this maximum under the assumption of constant body size and re-entry angle.⁹ The flight conditions for peak heating are related to, but not necessarily identical with, those for peak deceleration. In what follows, we determine the conditions for peak heating for any given heating rate, relate them to the ballistic parameter ($M/C_D A$), and determine the mass of ablated material consonant with the simplifying assumptions.

Ignoring the gravitational attraction, which is justified for large decelerations at steep angles, the deceleration of a body of mass M and frontal area A , having a drag coefficient C_D , is

$$M dV_\infty / dt = -\frac{1}{2} \rho_\infty V_\infty^2 C_D A \quad (2.1)$$

in which ρ_∞ is the atmospheric density and V_∞ the flight velocity. Assuming a straight-line trajectory near peak heating, inclined at an angle θ with the horizontal, the time rate of change of altitude z becomes

$$dz/dt = -V_\infty \sin \theta \quad (2.2)$$

To a good approximation, the atmospheric density varies exponentially with z , with a scale height l^* , determined by the altitude of peak heating^{††}

$$d \ln \rho_\infty / dz \equiv -1/l^* \quad (2.3)$$

** This assumption is contrary to the free-molecular situation, where the ablated mass is a strong radiator.

†† The range of l^* for $0 < z < 90$ km is approximately 7 km $< l^* < 12$ km.

By combination of Eqs (2.1-2.3), we find

$$\rho_\infty \phi d \ln V_\infty = -d\rho_\infty \quad (2.4)$$

where

$$\phi \equiv 2M \sin \theta / \rho_\infty l^* C_D A \quad (2.5)$$

If $M \sin \theta / C_D A$ is a constant along the trajectory,^{††} then Eq (2.4) may be integrated to give

$$V_\infty / V_\infty^* = \exp\{(1 - [\rho_\infty / \rho_\infty^*]) / \phi^*\} \quad (2.6)$$

the superscript asterisk denoting conditions evaluated at peak heating.

Whatever the cause of heating, the stagnation-point heat-transfer rate q will be some fraction ξ of the energy flux in the freestream:

$$q \equiv \frac{1}{2} \rho_\infty V_\infty^3 \xi \quad (2.7)$$

ξ will be determined by the mode of heating (convection or radiation), body size and shape, and the stagnation-point conditions that are related to the flight conditions by the assumption of equilibrium thermochemistry behind the bow shock. Following Chapman,⁹ we therefore propose that this detailed knowledge of the heat transfer (to be derived below) can be related to the flight conditions by a proportionality of the form

$$\xi \propto \rho_\infty^{-n} V_\infty^{-m} \quad (2.8)$$

For example, for free-molecule flow, $n = m = 0$, whereas both Chapman⁹ and Loh⁸ suggest $n = \frac{1}{2}$ and $m = 0$ for ballistic missile re-entry conditions.

In addition, whenever both convection and radiation are both important (but not necessarily simultaneous) contributors to the heating, we propose that the heat inputs of the form of Eqs (2.7) and (2.8) can be determined separately and then added to obtain the total heating. For any mode of heating, the proportionality constant of Eq (2.8) does not affect the flight conditions at peak heating but does, of course, determine the magnitude of the peak heat-transfer rate and, in this manner, also the amount of ablation. The body size and shape do not affect the value of m and n for any mode of heating, but do determine the relative importance of these various modes.

By combining Eqs (2.7) and (2.8), the condition that q have a maximum is found to be

$$d \ln V_\infty / d \ln \rho_\infty = (1 - n) / (m - 3) \quad (2.9)$$

But Eq (2.4) relates the logarithmic derivatives of V and ρ at peak heating, so that the value of ϕ^* is thereby determined to be

$$\phi^* = (3 - m) / (1 - n) \quad (2.10)$$

For the cases of free-molecule or ballistic missile conditions considered previously, ϕ^* is 3 or 6, respectively. For the meteor entry conditions considered in this paper, it is found below that ϕ^* lies between 1 and 20. For maximum deceleration, $\rho_\infty V_\infty^2$ must be a maximum according to Eq (2.1), and so also would be q if $n = 0$ and $m = 1$. Thus $\phi^* = 2$ would give identical flight conditions for peak deceleration and heating. For $\phi^* > 2$, peak heating occurs at higher altitudes than does peak deceleration.

For spherical meteors having a density of 3.2 g/cm³ (which is typical of stony meteors) and $C_D = 1$, the relationship between body radius R and ambient density and altitude at peak heating has been plotted in Fig. 1 by using Eq (2.5) and choosing a range of values of ϕ^* . The local scale height

†† For a sphere $M/C_D A$ is proportional to the radius. The constancy of $M \sin \theta / C_D A$, therefore, implies no great change in body radius.

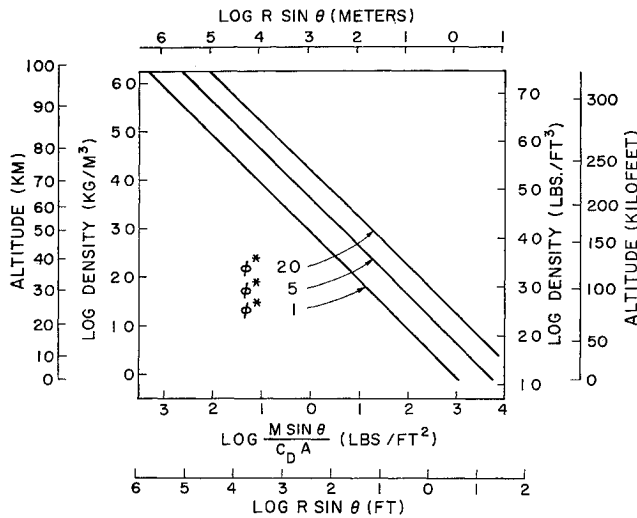


Fig 1 Altitude for peak heating as a function of ballistic parameter at various values of ϕ^* [cf Eq (2 5)] The values shown for $R \sin \theta$ correspond to a spherical body with a density of 3.2 g/cm^3 and $C_D = 1.0$

l^* and density as a function of altitude were determined from Ref 20

The total stagnation-point heat input Q may be obtained by integrating the instantaneous rate q along the trajectory:

$$Q = \int q dt = -2 \int_{V_{\infty}}^0 \frac{qM}{\rho_{\infty} V_{\infty}^2 C_D A} dV_{\infty} = - \int_{V_{\infty}}^0 \frac{\xi M}{C_D A} V_{\infty} dV_{\infty} \quad (2 11)$$

in which Eq (2 1) was used to convert the integral on time to one on velocity, V_{∞} being the initial velocity upon entry. Since the major contribution to this integral comes from an altitude variation of one scale height on either side of peak heating, we shall assume that $\xi M/C_D A$ has a constant value over the range of integration which is equal to its value at peak heating, so that by use of Eqs (2 6) and (2 7) the integral of Eqs (2 11) becomes, with $\rho_{\infty i} = 0$,

$$Q = \frac{1}{2} \xi^* (M/C_D A) (V_{\infty}^*)^2 \exp(2/\phi^*) \quad (2 12)$$

Neglecting the heat radiated from the body or stored in the body compared with the heat transferred to it, the latter then will be absorbed by ablation. In accordance with the usual assumptions regarding ablation,⁸ the total ablated mass ΔM is related to the total heat transfer Q by

$$\Delta M = fQA/[\Delta h + \frac{1}{2}\eta(V_{\infty}^*)^2] \quad (2 13)^{\S\S}$$

in which f is the ratio of total heat transfer to the product of stagnation-point heat input (Q) times frontal area (A), Δh is the heat per unit mass required to vaporize the material or to melt it, and η is $\frac{2}{3}$ for a vaporizing laminar boundary layer¹⁰ or zero for a nonvaporizing layer.¹¹ In the case where the material vaporizes, Δh is taken to be the sum of the heat of vaporization, the heat of fusion, and the heat capacity of the material, calculated in the present analysis for a temperature rise to melt of 1800°K . (This value of Δh would be approximately that corresponding to sublimation as well.) If the material only melts, then Δh is the sum of the heat of fusion and heat capacity of the material only.

^{\S\S} According to Eq (2 13), although the effective heat of absorption of the ablating material $\Delta h + \eta(V_{\infty}^*)^2/2$ increases with velocity, the ablated mass also increases with velocity, since the heat transfer increases more rapidly than $(V_{\infty}^*)^2$.

^{\S\S} The quantity η measures the blowing effect of the vaporizing material in reducing the heat input to the solid surface of the body.

The value of $\frac{2}{3}$ for η has been determined for lower-speed ablation processes, and we suppose it to be approximately correct at meteoric velocities. Whether the ablation process is fundamentally different at very high velocities is, of course, open to question and can only be resolved by further studies. For example, the spalling of stony meteorites would not only require $\eta = 0$, since there is no blowing effect, but also would reduce Δh to be less than its value for melting.

The effect of boundary-layer "blowing" also might be present in the case of radiant heating, provided the boundary-layer material was opaque to the incident radiation so that the net heat to reach the solid surface would have to be conducted through the boundary layer. For this reason, we have included this possibility in the subsequent study of radiant heating by setting $\eta = \frac{2}{3}$ for an opaque, vaporizing boundary layer. This point is discussed further at the end of Sec V.

By combination of Eqs (2 12) and (2 13), the fractional mass loss becomes

$$\frac{\Delta M}{M} = \frac{f\xi^*(C_D^*)^{-1} \exp(2/\phi^*)}{\eta + [2\Delta h/(V_{\infty}^*)^2]} \quad (2 14)$$

Of course, if $\Delta M/M$, calculated in this manner, were found to be close to or larger than unity, then the initial assumptions regarding the constancy of $\xi M/C_D A$ used in Eqs (2 6) and (2 11) are no longer valid, and Eq (2 14) is no longer meaningful. However, Eq (2 14) does provide a consistent criterion for nearly intact survival, say $\Delta M/M \leq \frac{1}{2}$, which implies that the body radius does not change by more than 20%. This is sufficiently close to the constant body radius required for all the integrations so as to make Eq (2 14) a reasonably good estimate of the mass loss.

III Equilibrium Stagnation-Point Properties

As a first step in the quantitative estimate of meteor dynamics and thermodynamics, an altitude-velocity diagram (Fig 2) was prepared, covering the complete velocity range for bodies originating within the solar system (10–70 km/sec, approximately), and altitudes from sea level to 90 km. The stagnation temperature (T_s , $^\circ\text{K}$), electron density (n_e , number/cm³), and average ionic charge (Z_e) shown are for equilibrium air behind a stationary normal shock with an upstream velocity corresponding to that shown on the abscissa.

The freestream density variation with altitude was found using the 1959 ARDC Standard Atmosphere,²⁰ and the equilibrium thermodynamic properties behind the shock were computed from the data of Ref 12 using the hypersonic approximation that

$$H_s = V_{\infty}^2/2 \quad p_s = \rho_{\infty} V_{\infty}^2 \quad (3 1)$$

in which H_s and p are the stagnation enthalpy and pressure, respectively. Equations (3 1) are sufficient to define completely the equilibrium thermodynamic state within the shock layer. From Ref 12, the temperature, density, and molal composition may be found directly. The average ionic charge Z_e was found from

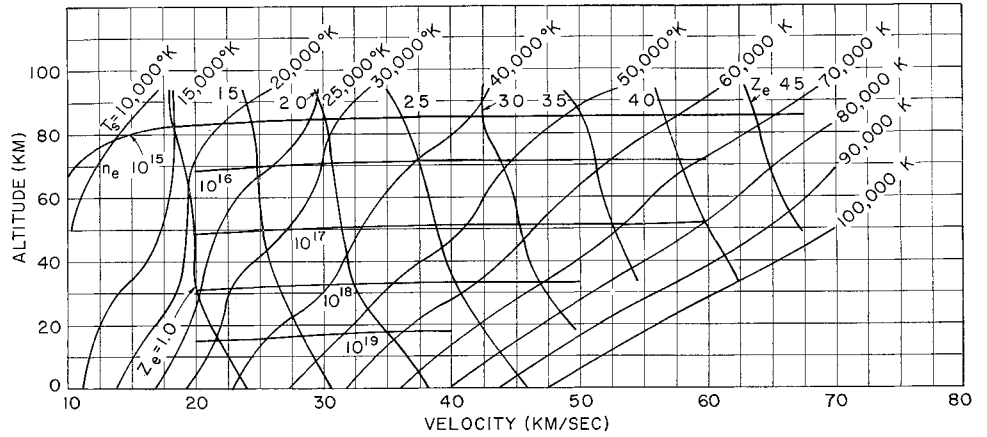
$$Z_e = (Z - 2)/2 \quad p = \rho ZRT \quad (3 2)$$

where Z is the total molal concentration as given by the perfect gas law.

IV Convective Heat Transfer

Examination of Fig 2 reveals that for velocities in excess of about 20 km/sec the shock-heated air in the stagnation region may be treated as a multiply ionized gas. The detailed treatment of convective heat transfer from such a gas is a problem of considerable complexity; however, a number of assumptions can be made which render the problem tract-

Fig 2 Equilibrium stagnation temperature T_s (K), electron number density n_e (cm^{-3}), and average ionic charge Z_s for a blunt body as a function of flight velocity and altitude. Thermodynamic data were taken from Ref 12



able The heat flux to the wall may be written as

$$q = -K_w(\partial T/\partial y)_w \quad (4.1)$$

where K_w is the thermal conductivity of the gas at the wall, and $(\partial T/\partial y)_w$ is the temperature gradient at the wall. If it is assumed that the electrons and ions are in equilibrium at the same temperature, that the composition remains constant through the boundary layer,** and that the perfect gas law applies, the expression for this stagnation-point heat transfer to the wall may be written as¹³

$$q = \left[2C_p K \rho \left(\frac{du}{dx} \right) \right]^{1/2} T \left[\frac{K \rho}{K \rho} \frac{d\theta}{d\eta} \right]_w \quad (4.2)$$

where

$$\theta \equiv T/T_s \quad (4.3)$$

$$\eta \equiv \left[\frac{2\rho C_p}{K} \left(\frac{du}{dx} \right) \right]^{1/2} \int_0^y \theta^{-1} dy \quad (4.4)$$

In these relations, C_p and T are the gas specific heat at constant pressure and temperature, respectively, and du/dx is the gradient of the velocity parallel to the surface in the inviscid flow external to the boundary layer. The subscripts s and w refer to stagnation and wall conditions, respectively.

The stagnation-point velocity gradient (du/dx) appearing in Eqs (4.2) and (4.4) is given by the Newtonian approximation as

$$(du/dx) = (2p/\rho)^{1/2}/R \quad (4.5)$$

$$= (V_\infty/R)(2\epsilon)^{1/2} \quad (4.6)$$

where

$$\epsilon \equiv \rho_\infty/\rho \quad (4.7)$$

and R is the radius of curvature of the body at the stagnation point. The Newtonian approximation is empirically valid for sphere-like bodies¹⁴

For an ionized plasma,¹⁷ K varies as $T^{5/2}$, so that

$$K/K = \theta^{5/2} \quad (4.8)$$

Equation (4.2) may then be rewritten as

$$q = \left[\frac{2V_\infty}{R} (2\epsilon)^{1/2} \frac{K \rho}{C_p} \right]^{1/2} C_{ps} T \left[\theta^{3/2} \frac{d\theta}{d\eta} \right]_w \quad (4.9)$$

To evaluate the temperature gradient at the wall, we introduce the simplification that the boundary layer across

*** This implies that the gas is not deionized at the body surface. For the stagnation conditions considered the thermal enthalpy and ionization enthalpy are about equal, so that the heat transfer would be higher if deionization occurs.

which the heat is transferred is an essentially inviscid thermal layer. This results from the fact that, in a multiply ionized boundary layer, the high electron mobility leads to a high thermal conductivity (and thus low effective Prandtl number), so that the thermal boundary-layer thickness is large compared to the viscous layer thickness. Since the flat plate and stagnation-point laminar boundary-layer energy equations are equivalent for inviscid flows, the results of a numerical integration of the former performed by Jepson¹⁵ may be used to evaluate the wall-temperature gradient appearing in Eq (4.9).

This analysis shows that

$$[\theta^{3/2}(d\theta/d\eta)]_w = 0.38 \quad (4.10)$$

For a more general expression for this term, see Ref 16.

In dimensionless form, the stagnation-point convective heating is thus given by

$$\begin{aligned} \xi &= \frac{q_s}{\frac{1}{2}\rho_\infty V_\infty^3} \\ &= 0.64 \left\{ \frac{K_s}{\epsilon^{1/2} R V_\infty \rho_\infty C_{ps}} \right\}^{1/2} \left\{ \frac{C_{ps} T_s}{V_\infty^2/2} \right\} \end{aligned} \quad (4.11)$$

where C_p may be conveniently found from

$$C_p = \frac{5}{2} (k/m_i) (1 + Z) \quad (4.12)$$

in which k is Boltzmann's constant and m_i the ionic mass.

For the present calculations, the thermal conductivity K was found using Spitzer's expression for a fully ionized plasma¹⁷

$$K = 4.67 \times 10^{-2} \frac{\delta_T T^{5/2}}{Z \ln \Lambda} \frac{\text{cal}}{\text{sec-cm}^2 \text{K}} \quad (4.13)$$

where

$$\Lambda = (3/2Z e^3) (k^3 T^3 / \pi n)^{1/2} \quad (4.14)$$

and in which e is the magnitude of the electronic charge, and δ_T varies from 0.22 to 0.52 as Z varies from one to infinity.¹⁷

A comparison of the results of Eq (4.11) can be made with the more detailed calculations of Kemp and Fay.¹³ Such a comparison is shown in Fig 3 for $V_\infty = 20$ km/sec, where $\xi^*(\sin\theta)^{-1/2}$ is plotted (solid line) as a function of $\log R \sin\theta$. Here the density and altitude, which correspond to the values of $R \sin\theta$ in the abscissa, are obtained from the peak heating curves of Fig 1. The curve of $\phi^* = 5$ in Fig 1 corresponds to the case of peak convective heating, as will be shown in Sec VI. The calculations of Fay and Kemp include the effects of deionization and atomic recombination on the wall, giving higher heat transfer than the present approximation, which ignores these effects. No equivalent calculations for higher flight velocities have yet been reported.

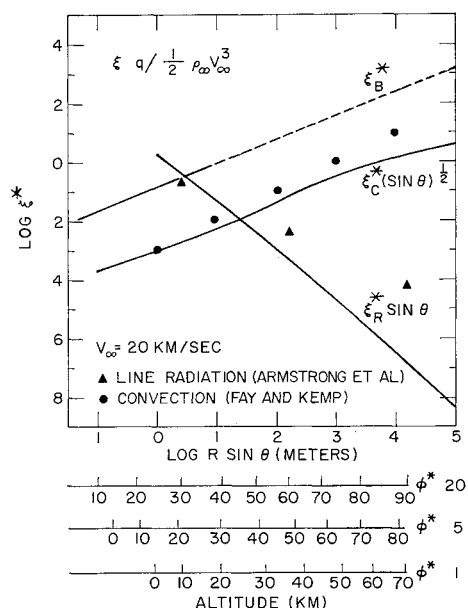


Fig 3 Dimensionless radiative and convective heat-transfer rates at peak heating as a function of body size for $V_\infty = 20$ km/sec. The altitude scales on the abscissa correspond to the curves of Fig 1. Shown for comparison are line radiation estimates of Armstrong et al.²² (compare with $\xi_R^* \sin \theta$) and the results of a more exact calculation of the convective heat flux by Kemp and Fay¹³ [compare with $\xi_c^* (\sin \theta)^{-1/2}$].

V Radiative Heat Transfer from Air Gas Cap

For equilibrium stagnation conditions at velocities in excess of 20 km/sec there will be no molecular species, but only ions (singly or more ionized) and electrons in the air gas cap. The radiation will consist of spectral lines of the various ions which may be appreciably Stark-broadened¹⁸ at high electron densities, and a continuum due to free-bound and free-free transitions of the electrons colliding with ions. Since the integrated line emission is proportional to the ion density while the continuum emission is proportional to the product of ion and electron densities, the ratio of the latter to the former increases with increasing density.

It is convenient to consider two extreme cases for which it is possible to calculate limits of radiant heat transfer. For a transparent gas, there is no reabsorption of the emitted radiation within the gas sample. For the continuum radiation, it is therefore sufficient that the photon mean free path l_p be much greater than the shock-layer thickness Δ . Under such conditions, the radiant heat transfer to the body at the stagnation point q_R is one-half the total emission, as determined in Eq (A17) of the Appendix:

$$q_R = 2\sigma T^4 \Delta / l_p$$

$$\xi_R = 2q_R / \rho_\infty V_\infty^3 = 4\sigma T^4 \Delta / \rho_\infty V_\infty^3 l_p \quad (51)$$

where the Planck mean free path for the continuum radiation l_p is given by Eq (A18) of the Appendix and where Δ is taken equal to $R/10$ (see Sec VI). The values of l_p so calculated for stagnation conditions at $V_\infty = 20$ and 70 km/sec are plotted in Fig 4 as a function of altitude. By comparison with the curves for body radii having peak heating at the same altitude, it can be seen that the condition for a transparent nose cap $l_p > \Delta$ obtains for body radii less than about 1 m. It will be shown in Sec VI that the curve $\phi^* \approx 1$ corresponds to peak transparent radiative heating.

For line radiation, an upper limit is found by assuming no reabsorption at the line centers, and calculating the total emission from known or estimated oscillator strengths. A calculation of the latter type by Armstrong et al.²² is com-

pared in Fig 3 with the continuum emission given by Eq (51), the comparison being made at values of Δ and ρ_∞^* determined by the peak heating analysis (see curve for $\phi^* = 1$ in Fig 1). It can be seen that the maximum line radiation heating (triangular points in Fig 3) exceeds the continuum radiation heat transfer ($\xi_R^* \sin \theta$) only for small bodies for which the convective heat transfer (ξ_c^*) is the major heating mechanism, and that the line and continuum heating are about equal at the altitude for which the gas cap becomes opaque to continuum radiation. Thus the upper and lower limits of transparent radiation are defined for peak heating conditions, but only an analysis of the line-broadening effects can determine under what conditions the upper limit can be reached.

The opposite extreme of an opaque gas also lends itself readily to analysis. For continuum radiation, if the photon mean free path is sufficiently small, the radiation thermal conductivity K_R , as given by Eq (A12), may be used in place of K_s in Eq (411) of the convective heat-transfer analysis in order to find the heat transfer due to diffusion of radiation. However, this is correct only if the Rosseland mean free path, $\dagger\dagger\dagger$ Eq (A14), is less than the boundary-layer thickness, computed in the usual manner, but with K_R replacing the gas kinetic thermal conductivity. Computing l_R from Eq (A14) in the Appendix, we have found that this condition never obtains for bodies which are small enough to experience peak heating above sea level. Since survival is usually assured for bodies larger than this, the radiation conductivity limit is not pertinent to our study $\dagger\dagger\dagger$.

There is a range of conditions for which the photon mean free path is less than the shock-layer thickness, but larger than the calculated radiation boundary-layer thickness. (This situation is quite analogous to the hypersonic rarefied gas flow for which the kinetic mean free path behind the bow shock is smaller than the shock-layer thickness, but larger than the computed viscous-layer thickness.) Under these conditions, an upper limit to the radiant heating is clearly

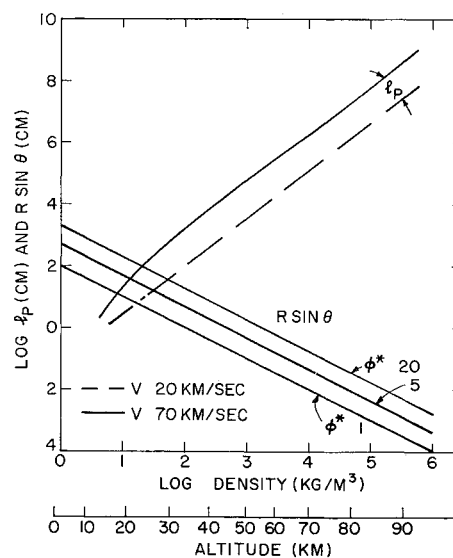


Fig 4 The Planck mean free path for continuum radiation (l_p) at stagnation conditions compared with the body size having peak heating at the same altitude (Curves for $R \sin \theta$ were taken from Fig 1).

$\dagger\dagger\dagger$ For stagnation conditions, the Planck and Rosseland mean free paths are approximately equal.

$\dagger\dagger\dagger$ Although line radiation decreases l_R below the value for the continuum alone, it is less important at the high densities which are needed for the opaque limit to be reached. Consequently, we expect that it would not significantly alter the value of l_R used in arriving at the conclusion given.

Table 1 Values of n , m , and ϕ^* for convective and radiative heat-transfer modes

Mode	n	m	ϕ^*
Laminar convection	0.33	-0.37	5
Transparent radiation	-0.79	0.7	1.2
Blackbody radiation	0.79	-1.0	19

the blackbody limit:

$$\xi_B = 2\sigma T^4 / \rho_\infty V_\infty^3 \quad (5.2)$$

which has been plotted in Fig. 3 for peak heating conditions. For blackbody radiation this corresponds to $\phi^* \approx 20$, as will be shown in Sec. VI. This opaque limit and the transparent limit of the continuum radiation of Eq. (5.1) are equal at $l_p = 2\Delta$. Although a smooth transition from one limit to the other could be devised along the lines suggested by Probst, we have not considered such a refinement. The peak convective and radiative heating are also plotted for $V_\infty = 70$ km/sec in Fig. 5. The curves of Figs. 3 and 5 bear out the original assumption of small radiation cooling behind the bow shock.

VI Heat Fluxes at Peak Heating

It can be seen from Eqs. (4.11) and (5.1) that the convective and transparent radiative heat fluxes have an explicit dependence on the body size R . (In the latter case, the shock-detachment distance Δ is approximately ϵR for a spherical body¹⁴). If, however, only the peak heating region is considered, there is a direct correspondence between R and ρ_∞^* (and hence altitude) for constant ϕ^* as shown in Fig. 1, so that ξ_c^* and ξ_R^* may be computed as functions of altitude for selected values of ϕ^* and velocity. The values of n and m which determine the proper value of ϕ^* to be used for a particular mode of heating, according to Eq. (2.10), can be found by noting that

$$n = -\left(\frac{\partial \ln \xi}{\partial \ln \rho_\infty}\right)_{V_\infty, R} \quad m = -\left(\frac{\partial \ln \xi}{\partial \ln V_\infty}\right)_{\rho_\infty, R} \quad (6.1)$$

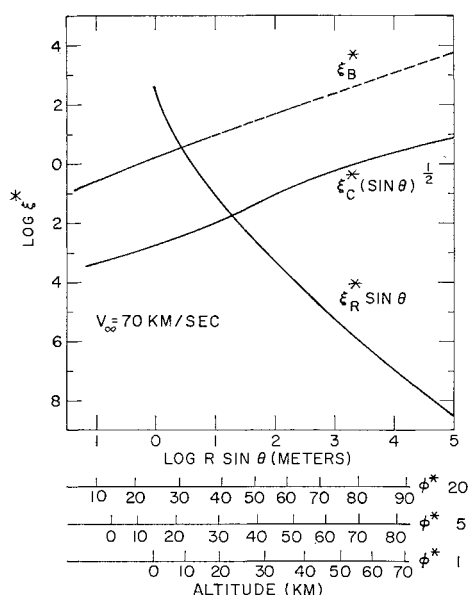


Fig. 5 Dimensionless radiative and convective heat-transfer rates at peak heating as a function of body size for $V_\infty = 70$ km/sec. The altitude scales on the abscissa correspond to the curves of Fig. 1.

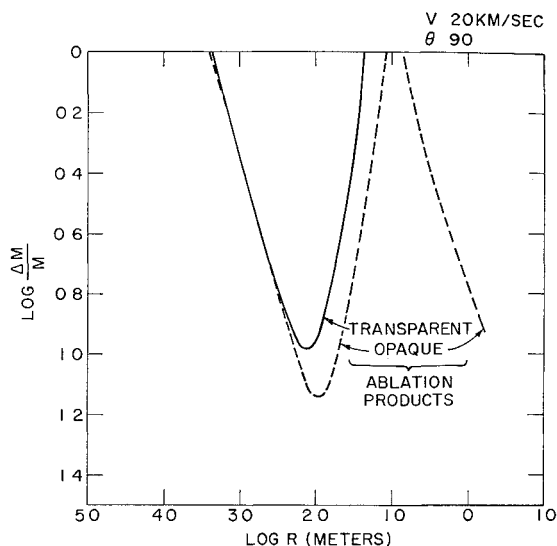


Fig. 6 Fractional mass loss for vaporizing body as a function of body size for vertical entry and $V_\infty = 20$ km/sec. The physical properties of the body are those used in Fig. 1.

As a typical case, the spherical body used in the calculations of Fig. 1 was considered, with $\epsilon = 1/10$ so that $\Delta = R/10$. Values of ξ^* , ξ_R^* , and ξ_B^* were computed for 20 and 70 km/sec over an altitude range from sea level to 90 km and for several assumed values of ϕ^* . From these results, and noting that

$$\left(\frac{\partial \ln \xi}{\partial \ln \rho_\infty}\right)_{V_\infty, R} = \left(\frac{\partial \ln \xi}{\partial \ln \rho_\infty}\right)_{V_\infty, \phi^*} - \left(\frac{\partial \ln \xi}{\partial \ln R}\right)_{V_\infty, \rho_\infty} \left(\frac{\partial \ln R}{\partial \ln \rho_\infty}\right)_{\phi^*} \quad (6.2)$$

it was possible to find n , m , and the appropriate value of ϕ^* for each mode of heat transfer. The results are shown in Table 1.

The computed values of ξ_c^* , ξ_R^* , and ξ_B^* corresponding to the appropriate value of ϕ^* are shown in Figs. 3 and 5 as functions of $R \sin \theta$ for $V_\infty = 20$ and 70 km/sec, respectively. Also shown on the abscissa are the altitudes of peak heating for the associated value of $R \sin \theta$ at $\phi^* = 1, 5$, and 20. Thus, the maximum convective, transparent, and blackbody radiative heating for a particular $R \sin \theta$ will occur approximately at the altitude given by the $\phi^* = 5, 1$, and 20 coordinates, respectively.

Using the results presented in Figs. 3 and 5, calculations of the fractional mass loss given by Eq. (2.14) were made for several cases. The body was assumed to be stone-like, with a value of Δh for vaporization of 1.89 and 0.459 kcal/g for melting, §§§ a density of 3.2 g/cm³, and a drag coefficient of unity. The value of ξ^* used was the sum of the radiative and convective contributions, the former being the transparent or blackbody value depending upon whether the altitude was, respectively, above or below that altitude at which $\Delta = l_p/2$. For each velocity and entry angle, three regimes were considered: 1) no vaporization, and hence no blowing ($\eta = 0$), 2) vaporization, with transparent ablation products ($\eta = \frac{2}{3}$ for the convective contribution and $\eta = 0$ for the radiative contribution), and 3) vaporization with opaque ablation products ($\eta = \frac{2}{3}$ for both contributions). The results of these calculations are shown in Figs. 6-8. In each

§§§ The heat capacity of the material was based on a temperature rise to melt of 1800°K and a specific heat of 9×10^4 erg/g. The heat of fusion was taken as 0.072 kcal/g, and the heat of vaporization as 1.43 kcal/g (see Ref. 7, p. 161).

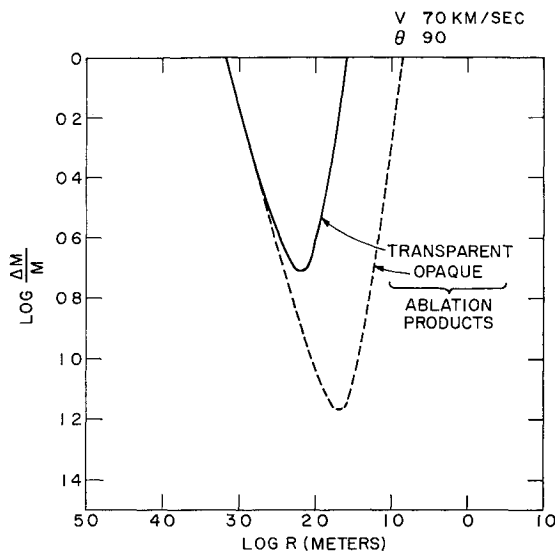


Fig 7 Fractional mass loss for vaporizing body as a function of body size for vertical entry and $V_\infty = 70$ km/sec. The physical properties of the body are those used in Fig 1

case, the left-hand portion of the curve corresponds to those body sizes whose peak heating is predominantly convective, and the central portion between the peaks to those for which transparent radiation is dominant. At the largest values of R , l_p at the peak heating altitude becomes smaller than Δ , and the radiative heating (and therefore $\Delta M/M$) corresponds to that given by the blackbody limit.

VII Discussion

From the curves for the radiative and conductive heat-transfer coefficients plotted for homogeneous stony meteors in Figs 3 and 5, we may conclude that the convective and transparent radiative coefficients are practically independent of velocity, at least in the range of 20–70 km/sec. In addition, from the relative magnitudes of the transparent radiative coefficient and the convective coefficient, we can also conclude that radiation heating will only become important at altitudes below 25 km, at which point the shock layer is optically thin. Only for bodies having peak heating within a scale height above sea level will the gas cap become opaque, and, even in this region, the diffuse radiation approximation for heat transfer to the body is not applicable for reasons mentioned in Sec V.

Of more direct significance are the mass loss calculations that have been carried out using the computed heat-transfer coefficients. These results are shown for vaporizing bodies in Figs 6 and 7 for vertical entry at 20 and 70 km/sec, and in the case of 20 km/sec also for entry at 30° in Fig 8. The ordinate on these curves is the relative mass loss. Since the meteor radius is assumed to be approximately constant during entry, the results can be considered meaningful for $\Delta M/M$ less than, say, $\frac{1}{2}$, although, even for larger values of $\Delta M/M$, the curves do give an indication of the relative mass loss. One of the interesting general features of the results is the relatively weak velocity dependence (between 20 and 70 km/sec) for the surviving ablating bodies, as well as the relatively small effect of entry angle (so long as it is sufficiently steep).

Although not shown on Figs 6–8, the calculations indicate that the nonvaporizing body will not survive, in the sense that we have defined survival, unless it is large enough not to experience peak heating above sea level (see Fig 1). In order to survive a vertical entry within our terms of reference, a nonvaporizing body must be larger than about 10 m. This

conclusion is not substantially changed by a different entry angle.

The minimum in the mass loss curves of Figs 6–8 occurs at the point where convection and transparent radiation heating are equal. This minimum is sufficiently low to insure survival of bodies between a fraction of a centimeter to several centimeters in radius, essentially irrespective of velocity or entry angle. If an ablating boundary layer is opaque, the size range for survival is somewhat increased, and more so at the higher speeds. Figures 6 and 8 also indicate that, if the ablation products are opaque to the gas-cap radiation, then bodies larger than 0.5 m may also survive for entry speeds between 20 and 40 km/sec. The survival of very small bodies (fraction of a millimeter) is determined by free-molecule processes not considered here, whereas very large bodies (greater than 10 m) will survive by virtue of failing to pass through peak heating above sea level.

The failure of nonvaporizing bodies to survive may, to some extent, account for the large ratio of stone meteors to iron meteors found on the earth's surface if it is assumed that the former vaporize whereas the latter do not. Of course, the distinction between metallic materials which melt without vaporizing and glassy materials which vaporize with little melting is one derived from ballistic-missile velocity ablation experiments, and may not exist under conditions of higher velocity. Furthermore, the possibility of spalling of stone meteors may also be important in this comparison.

The preceding results concerning survival do not agree with those of Riddell and Winkler,³ who indicate that meteors whose radius on entry is in the range of 0.5 cm to about 50 m will not survive in the sense we have been referring to. A direct comparison of the results of the present analysis with those of Allen^{4,6} is not possible, as his calculations were presented for velocities lower than those here.

An interesting analysis of the Meanook 132 meteor data by Allen and Yoshikawa⁵ showed that the mean body radius (assuming 1 g/cm³ body density) decreased from about 6 to 3 cm between 70 and 44 km, at which point the meteor broke into pieces. This approximately ten-to-one reduction in mass ($\Delta M/M \approx 0.9$) is consistent with the curve of Fig 8 for a vaporizing body with a transparent boundary layer, assuming that $R = 6$ cm.

If deceleration and luminosity data on meteors that do survive were available, a much more detailed comparison with the data of both the present and other theories would be possible. In particular, much information as to the validity of the present theory could be determined from peak heating (which may be associated with peak luminosity) and peak deceleration data. In addition, the recovery of such meteors would provide one more piece of added information that presently does not exist in connection with meteor records.

Appendix: Planck and Rosseland Mean Free Paths for Continuum Radiation

The energy radiated in free-free and free-bound collisions of electrons with hydrogen-like ions, in a plasma having a Boltzmann electron velocity distribution of temperature T , is given by Brussard and van de Hulst²³ as

$$\epsilon = \frac{32\pi}{3(3)^{1/2}} \frac{Z^2 e^6}{m^2 c^3} \left(\frac{2\pi m}{kT} \right)^{1/2} n_e n_i G \quad (A1)$$

where

$$G \equiv \left(1 + 2\theta \sum_{n=1}^{\infty} n^{-3} e^{\theta/n^2} \right) e^{-h\nu/kT} \quad (A2)$$

and

$$\theta = \frac{2\pi^2 m e^4 Z^2}{h^2 kT} \quad (A3)$$

and in which ϵ is the energy radiated per unit volume, time, and frequency, ν is the frequency, m is the electron mass, e the electronic charge, Z the ionic charge, n_i and n are the ionic and electron number densities, n is the principal quantum number, and θ is the ratio of ion-electron recombination energy to kT . If we define an ionization frequency ν_i by

$$h\nu_i = 2\pi m e^4 Z^2 / h^2 = \theta kT \quad (\text{A4})$$

then the smallest quantum number n_m defining the lower limit in the sum of Eq (A2) is an integer such that

$$n_m^2 \geq \nu_i / \nu \quad (\text{A5})$$

In Eq (A1), the Gaunt factor²³ is assumed to be unity

Menzel and Pekeris²⁵ have suggested an approximation to the sum in Eq (A2) which consists in replacing it by an integral with a limit given by the equality of Eq (A5). As pointed out by Brussard and van de Hulst,²³ this smoothing of the spectral variation of ϵ_ν is a good approximation for all frequencies if $h\nu_i \ll kT$, but otherwise only for frequencies for which $h\nu \ll kT$. The approximation becomes

$$\begin{aligned} 2\theta \sum_{n_m}^{\infty} \frac{e^{\theta/n^2}}{n^3} &\simeq 2\theta \int_{n_m}^{\infty} \frac{e^{\theta/n^2}}{n^3} dn \\ &\simeq e^{h\nu/kT} - 1 \quad \text{if } \nu < \nu_i \\ &\simeq e^{h\nu_i/kT} - 1 \quad \text{if } \nu > \nu_i \end{aligned} \quad (\text{A6})$$

in which the equality of Eq (A5) was used when $n_m > 1$, but $n_m = 1$ for $\nu > \nu_i$. Equation (A2) is then approximated by

$$\begin{aligned} G &\simeq 1 \quad \text{if } \nu < \nu_i \\ &\simeq \exp[-h(\nu - \nu_i)/kT] \quad \text{if } \nu > \nu_i \end{aligned} \quad (\text{A7})$$

A mean free time for a photon τ_ν may be defined as the ratio of the equilibrium energy density of the radiation field to the energy radiated, ϵ_ν , or

$$\tau_\nu = \frac{8\pi h\nu^3}{c^3(e^{h\nu/kT} - 1)\epsilon_\nu} \quad (\text{A8})$$

The photon mean free path l_ν becomes

$$\begin{aligned} l &\equiv c\tau_\nu \\ &= \frac{3m c h\nu^3}{4n n_i Z^2 e^8} \left(\frac{3m kT}{2\pi} \right)^{1/2} (e^{h\nu/kT} - 1)^{-1} G^{-1} \end{aligned} \quad (\text{A9})$$

The Rosseland mean free path l_R is defined by²¹⁻²⁵

$$l_R = \frac{15}{4\pi^4} \int_0^\infty \frac{l_\nu x^4 e^x}{(e^x - 1)^2} dx \quad (\text{A10})$$

where

$$x \equiv h\nu/kT$$

This definition results from observing that the radiation thermal conductivity K_R , which is given by²⁴

$$K_R = \frac{c}{3} \int_0^\infty l_\nu \frac{d}{dT} \left\{ \frac{8\pi h\nu^3}{c^3(e^{h\nu/kT} - 1)} \right\} d\nu \quad (\text{A11})$$

becomes the Rosseland value for a gray gas of mean free path l_R :

$$K_R = 16(\sigma T^3 l_R)/3 \quad (\text{A12})$$

where

$$\sigma \equiv 2\pi^5 k^4 / 15 h^3 c^2 \quad (\text{A13})$$

when Eq (A10) is substituted in Eq (A11)

Inserting Eq (A9) into Eq (A10), l_R becomes

$$l_R = \frac{45}{32\pi^4} \frac{mc(kT)^3}{n_i n_e Z^2 e^8 h^2} \left(\frac{6mkT}{\pi} \right)^{1/2} \int_0^\infty \frac{x^7 e^x dx}{(e^x - 1)^3} \quad (\text{A14})$$

¶¶¶Menzel and Pekeris²⁵ do not remark on the variation of G with ν when $\nu > \nu_i$

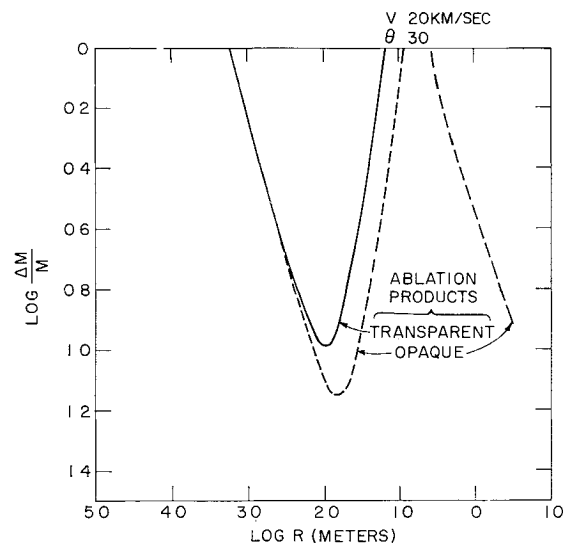


Fig 8 Fractional mass loss for vaporizing body as a function of body size for $\theta = 30^\circ$ and $V_\infty = 20$ km/sec. The physical properties of the body are those used in Fig 1

provided that $G = 1$ for all values of ν . Since the contribution to l_R for $\nu > \nu_i$ is exponentially small, this approximation, which removes ν_i as an argument in l_R , is quite accurate. The definite integral in Eq (A14) has a value of 22.6

For a thin transparent slab of gas of thickness Δ , the rate of energy loss per unit area and frequency in both directions, $\epsilon \Delta$, is

$$\epsilon_\nu \Delta = \frac{8\pi h\nu^3 \Delta}{c^2(e^{h\nu/kT} - 1)l_\nu} \quad (\text{A15})$$

by virtue of Eq (A8). Defining the Planck mean free path l_p by

$$l_p^{-1} = \frac{15}{\pi^4} \int_0^\infty \frac{l_\nu^{-1} x^3 dx}{e^x - 1} \quad (\text{A16})$$

the integration of Eq (A15) over all frequencies gives

$$\Delta \int_0^\infty \epsilon d\nu = \frac{4}{l_p} \Delta \sigma T^4 \quad (\text{A17})$$

Substituting Eq (A9) into Eq (A16), l_p becomes

$$l_p = \frac{\pi^3}{20} \frac{m c (kT)^3}{n_i n_e Z^2 e^8 h^2} \left(\frac{3\pi m kT}{2} \right)^{1/2} \left(\frac{h\nu_i}{kT} + 1 \right)^{-1} \quad (\text{A18})$$

with the result that

$$l_R = 0.134[(h\nu_i/kT) + 1]l_p \quad (\text{A19})$$

Equations (A14) and (A18) for l_R and l_p differ somewhat from the expressions of Pappert and Penner²¹ for an equilibrium multiply ionized plasma. They first averaged l_ν over the equilibrium population of species and then over frequency, arriving at a result which does not differ from the preceding by more than a factor of 2 if Ze is interpreted as the average charge per ion. The numerical values also agree, within the same accuracy, with the continuum calculation of Armstrong et al.²² Equation (A14) is identical to that derived by Menzel and Pekeris²⁵

References

- Hansen, C. F., "The erosion of meteors and high speed vehicles in the upper atmosphere," NACA TN 3962 (1957)
- Gazley, C., Jr., "Meteoric interaction with the atmosphere; theory of drag and heating and comparison with observations,"

Rand Rept R-339, Rand Corp., Santa Monica, Calif (June 1959)

³ Riddell, F R and Winkler, H B, "Meteorites and re entry of space vehicles at meteor velocities," *ARS J* **32**, 1523-1530 (1962)

⁴ Allen, H J, "On the motion and ablation of meteoric bodies," *Aeronautics and Astronautics*, edited by N J Hoff and W G Vincenti (Pergamon Press Inc., New York, 1960), pp 378-416

⁵ Allen, H J and Yoshikawa, K K, "Luminosity from large meteoric bodies," *Smithsonian Contrib Astrophys* **7**, 181-193 (1963)

⁶ Allen, H J, "Hypersonic aerodynamic problems of the future," Fluid Mechanics Panel, AGARD, Brussels (April 3-6, 1962)

⁷ Opik, E J, *Physics of Meteor Flight in the Atmosphere* (Interscience Publishers Inc., New York, 1958), Chap 4

⁸ Loh, W H T, *Dynamics and Thermodynamics of Planetary Entry* (Prentice-Hall Inc., Englewood Cliffs, N J, 1963), p 184

⁹ Chapman, D R, "An approximate analytical method for studying entry into planetary atmospheres," *NACA TN* 4276 (1958)

¹⁰ Adams, M C, Powers, W E, and Georgiev, S, "An experimental and theoretical study of quartz ablation at the stagnation point," *J Aerospace Sci* **27**, 535-543 (1960)

¹¹ Howe, J T, "Radiation cooling of the stagnation region by transpiration of an opaque gas," *NASA TN* D-329 (1960)

¹² Anonymous, "The thermodynamic properties of high temperature air," Chance Vought Research Center Rept RE-1R-14 (June 1961)

¹³ Kemp, N H and Fay, J A, "Theory of stagnation-point heat transfer in a partially ionized diatomic gas," *AIAA J* **1**, 2741-2751 (1963)

¹⁴ Hayes, W D and Probst, R F, *Hypersonic Flow Theory* (Academic Press Inc., New York, 1959), p 243

¹⁵ Jepson, B M, "Heat transfer in a completely ionized gas,"

Magnetogasdynamics Rept 61-7, Dept Mechanical Engineering, Massachusetts Institute of Technology (July 1961)

¹⁶ Fay, J A, "Plasma boundary layers," *Magnetohydrodynamics, Proceedings of the Fourth Biennial Gas Dynamics Symposium* (Northwestern University Press, Evanston, Ill., 1962), p 342

¹⁷ Spitzer, L, *Physics of Fully Ionized Gases* (Interscience Publishers Inc., New York, 1956), p 87

¹⁸ Penner, S S, *Quantitative Molecular Spectroscopy and Gas Emissivities* (Addison-Wesley Publishing Co., Inc., Reading, Mass., 1959), pp 33-37

¹⁹ Probst, R F, "Radiation slip," *AIAA J* **1**, 1202-1204 (1963)

²⁰ Minzner, R A, Champion, K S W, and Pond, H L, "The ARDC model atmosphere 1959," Air Force Surveys in Geophysics 115, Air Force Cambridge Research Center 59 267, US Air Force, Bedford, Mass (August 1959)

²¹ Pappert, R A and Penner, S S, "Approximate continuous opacity calculations for polyelectronic atoms at high temperatures," *J Quant Spectry Radiative Transfer* **1**, 258-268 (1961)

²² Armstrong, B H, Sokoloff, J, Nicholls, R W, Holland, D H, and Meyerott, R E, "Radiative properties of high temperature air," *J Quant Spectry Radiative Transfer* **1**, 143-162 (1961)

²³ Brussard, P J and van de Hulst, H C, "Approximation formulas for nonrelativistic Bremsstrahlung and average Gaunt factors for a Maxwellian electron gas," *Rev Mod Phys* **34**, 507-519 (1962)

²⁴ Fay, J A, "Energy transfer in a dense plasma," *Propagation and Instabilities in Plasmas*, edited by W Futterman (Stanford University Press, Stanford, Calif., 1963), pp 103-114

²⁵ Menzel, D H and Pekeris, C L, "Absorption coefficients and hydrogen line intensities," *Monthly Notices Roy Astron Soc* **96**, 77-111 (1935); also preprinted in *Selected Papers on Physical Processes in Ionized Plasmas*, edited by D H Menzel (Dover Publications, Inc., New York, 1962), pp 3-37